Switch of encoding characteristics in single neurons by subthreshold and suprathreshold stimuli

Toshiaki Omori,[1,2] Toru Aonishi,[3,2] and Masato Okada[1,2,*]
[1]*Graduate School of Frontier Sciences, The University of Tokyo, Chiba 277-8561, Japan*
[2]*RIKEN Brain Science Institute, Saitama 351-0198, Japan*
[3]*Interdisciplinary Graduate School of Science and Engineering, Tokyo Institute of Technology, Kanagawa 226-8502, Japan*
(Received 1 November 2009; published 1 February 2010)

Spike-triggered analysis is a statistical method used to elucidate encoding properties in neural systems by estimating the statistical structure of input stimulus preceding spikes. A recent numerical study suggested that the profile of the spike-triggered average (STA) changes depending on whether the mean input stimuli are subthreshold or suprathreshold. Here we analytically verify the difference between subthreshold STA and suprathreshold STA by using the spike response model (SRM). We show by moment expansion that the suprathreshold STA is proportional to the first derivative of the response kernel, and that the subthreshold STA is expressed by a linear combination of the response kernel and its first derivative. We verify whether the analytical results obtained from the SRM can be applied to a multicompartment model with Hodgkin-Huxley type dynamics.

DOI: 10.1103/PhysRevE.81.021901 PACS number(s): 87.18.Sn, 87.19.lc

I. INTRODUCTION

Neurons are encoders that transform series of time-varying input stimuli into spikes. The spike-triggered analysis is a statistical method used to estimate the encoding properties of neurons by characterizing the statistical structure of the input stimuli inducing spikes [1–7]. In particular, the spike-triggered average (STA) and the spike-triggered covariance (STC), which are, respectively, the first and second moments of the spike-triggered ensemble, have been used extensively in recent experimental studies, in order to explore the receptive fields in neural systems [8–11].

The input-output relations of single neurons depend on the intrinsic dynamical properties governed by various ion channels, neuronal morphology, and so on. Hence, the intrinsic dynamical properties determine the encoding properties of single neurons. Several studies have tried to elucidate the relation between the encoding properties and the intrinsic dynamical properties quantitatively, by deriving the relation between the STA and the neural membrane dynamics analytically. Based on the stochastic process theory, the STA has been analytically calculated for simple neuron models such as the linear-nonlinear model [12], the phase oscillator model [13] and the threshold crossing model [14,15], as well as for more detailed neuron models such as the leaky integrate-and-fire model [16] and its generalized models [17–19].

Recently, Mato and Samengo [20] have shown by numerical simulations that in the theta model (also known as the Ermentrout-Kopell canonical model) [21,22] the profile of the STA differs depending on whether the mean stimuli to the neuron are subthreshold or suprathreshold. Their simulation results suggested that the STA is similar to the first derivative of the phase response curve (PRC) when the neuron receives the stimuli of suprathreshold mean, whereas the STA was suggested to resemble the PRC itself when the neuron receives the stimuli of subthreshold mean (in order to discriminate between these two kinds of STAs, we hereafter call the STA for subthreshold mean stimuli and that for suprathreshold mean stimuli as the subthreshold and suprathreshold STAs, respectively). This difference between the sub and suprathreshold STAs shown numerically implies that the encoding properties of neurons change depending on the average activity level. However, the difference between the sub and suprathreshold STAs has not been addressed in the previous analytical studies of the STA [12–19] while either the subthreshold STA [12,14–19] or the suprathreshold STA [13] was investigated in each of those studies. To show this difference analytically, we need to elucidate the relation between the STA and an intrinsic dynamical property other than the PRC, since the PRC cannot be defined when the neuron receives the subthreshold mean stimuli.

In this study, we analytically verify the difference between the sub and suprathreshold STAs shown numerically in the previous study [20], by analyzing spike response model (SRM) [23,24]. In the SRM, the intrinsic dynamical property is described by a response kernel (a linear response function) that can be defined regardless of whether the mean stimuli are subthreshold or suprathreshold. Moreover, the SRM is known to reproduce the intrinsic dynamical properties of biological plausible models such as the Hodgkin-Huxley model [25]. Here we show the analytical relation between the STA and the response kernel by analyzing the SRM. We first show a general form of the STA of the SRM by the moment expansion. Next, the suprathreshold STA is shown to be proportional to the first derivative of the response kernel by lower-order moment expansion, whereas the subthreshold STA is shown to be expressed by a linear combination of the response kernel and its first-order derivative by infinite-order moment expansion. By numerical simulations, we verify whether the analytical results obtained from the SRM can be applied to a multicompartment model with Hodgkin-Huxley type dynamics.

II. FORMULATION

In this section, we first describe the dynamics of the SRM and then relate the SRM to the STA.

*okada@k.u-tokyo.ac.jp

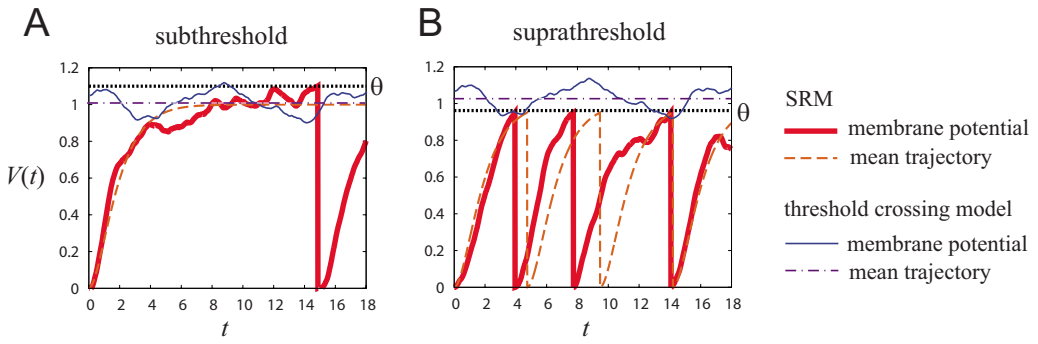

FIG. 1. (Color online) Time course of membrane potential in the SRM (thick solid line) and that in the threshold crossing model (thin solid line): (a) the case of subthreshold mean stimuli and (b) the case of suprathreshold mean stimuli. The mean trajectory of the SRM and that of the threshold crossing model are indicated by the dashed line (time varying) and dash dotted line (time constant), respectively. The firing threshold θ is shown by the dotted line.

A. Spike response model

We assume that the dynamics of membrane potential in single neurons obeys the SRM. In the SRM, the membrane potential $V(t)$ is expressed as follows [17]:

$$V(t) = \int_{\hat{t}}^{t} \kappa(t-s)I(s)ds + \eta(t-\hat{t}), \tag{1}$$

where $\hat{t}$ denotes the most recent firing time at time t. $\kappa(t)$ is the subthreshold response kernel describing the linear response to an input pulse, $I(t)$ is an external input current, and $\eta(t)$ is the suprathreshold response kernel describing the spike potential. Thus, in the SRM, the membrane potential is described as a sum of the suprathreshold response kernel $\eta(t)$ and a convolution of the subthreshold response kernel $\kappa(t)$ and an external input $I(t)$. Hereafter we call the subthreshold response kernel simply the response kernel. The firing time is defined as the time when the membrane potential crosses the firing threshold θ from below. The set of firing times, T_{spike}, is expressed as follows:

$$T_{\text{spike}} = \left\{ t \middle| V(t) = \theta \text{ and } \frac{dV(t)}{dt} > 0 \right\}. \tag{2}$$

We assume that the neuron receives a constant current I_0 and a stochastic current $\xi(t)$,

$$I(t) = I_0 + \xi(t), \tag{3}$$

where the stochastic current $\xi(t)$ is assumed to be a white Gaussian noise:

$$\langle \xi(t) \rangle_\xi = 0, \tag{4}$$

$$\langle \xi(t)\xi(t') \rangle_\xi = \sigma^2 \delta(t-t'). \tag{5}$$

$\delta(x)$ denotes Dirac's delta function and σ denotes the standard deviation of the white Gaussian noise.

We show a time course of membrane potential of the SRM in Fig. 1, in order to show the difference between the SRM used in this study and the threshold crossing model [21,22] used in the previous studies regarding the STA [14,15]. The thick solid line in Fig. 1(A) shows the membrane potential when the neuron receives the subthreshold mean stimuli. We find that the membrane potential fluctuates around the time-varying mean (dashed line). Note that the change in the mean of the membrane potential is due to the resetting mechanism in the SRM. On the other hand, the membrane potential in the threshold crossing model [thin solid line in Fig. 1(A)] fluctuates around the constant mean (dash dotted line), since threshold crossing model has no resetting mechanism (the threshold crossing model is equivalent to the SRM with the following two conditions: $\eta(t)$ =const and $\hat{t}=-\infty$). Thus, the threshold crossing model used in the previous studies [14,15] is a special case of the SRM used in the present paper. Since the mean of membrane potential in the SRM is time varying, its membrane potential [thick solid line in Fig. 1(B)] fluctuates *below* the firing threshold when the neuron receives the suprathreshold mean stimuli. Thus, the SRM can naturally treat the suprathreshold mean stimuli. In contrast, the threshold crossing model with the suprathreshold mean stimuli seems to be rather unnatural since its membrane potential [thin solid line in Fig. 1(B)] fluctuates *above* the firing threshold when the neuron receives the suprathreshold mean stimuli. We therefore use the SRM, which we can treat both the sub and suprathreshold mean stimuli.

B. Relating the spike-triggered average to the SRM

The STA is an ensemble average of time-varying current preceding each spike, and is defined as follows:

$$s(\tau) = \langle \xi(t_s - \tau) \rangle_\xi, \tag{6}$$

where t_s is a firing time. The average $\langle \cdot \rangle_\xi$ is taken with respect to time series of the stochastic current $\{\xi(t)\}$. In order to derive the STA of the SRM, we relate the first passage time of the SRM to the firing time, t_s, in the definition of the STA. The first passage time is defined as the time when a neuron passes a firing threshold from below for the first time [27]. When we assume that the first passage time of the neuron receiving the stochastic current $\{\xi(t)\}$ is determined by $f(t_s|\xi)$, the STA is expressed using $f(t_s|\xi)$ as follows:

$$s(\tau) = \left\langle \int_0^\infty dt_s f(t_s|\xi)\xi(t_s - \tau) \right\rangle_\xi, \tag{7}$$

$$f(t_s|\xi) = \Theta[V'(t_s)]\delta[V(t_s) - \theta]V'(t_s), \tag{8}$$

where $\Theta(x)$ is a Heaviside step function that takes a value of 1 for $x>0$, 1/2 for $x=0$, and 0 for $x<0$. The delta function $\delta[V(t_s)-\theta]$ and the Heaviside step function $\Theta[V'(t_s)]$ in the expression $f(t_s|\xi)$ restrict t_s to a firing time.

The method to relate the STA to the SRM [Eqs. (7) and (8)] described in the present subsection is equivalent to the one used to relate the STA to the threshold crossing model in the previous studies by Hong *et al.* [14] and Burak *et al.* [15].

III. SUB AND SUPRATHRESHOLD STAS OF THE SRM

We derive the relation between the STA and the SRM by using the moment expansion and we obtain the time profiles of the sub and suprathreshold STAs of the SRM analytically.

A. General form of the STA

The part of membrane potential driven by stochastic current $\xi(t)$ is expressed by the following equation:

$$v(t) = \int_{\hat{t}}^{t} \kappa(t-s)\xi(s)ds. \tag{9}$$

Using this expression, we express Eq. (8) as

$$f(t_s|\xi) = \Theta[v'(t_s) + H'(t_s)]\delta[v(t_s) + H(t_s)][v'(t_s) + H'(t_s)]. \tag{10}$$

where we put $H(t)$ as follows:

$$H(t) = I_0 \int_{\hat{t}}^{t} \kappa(t-s)ds + \eta(t-\hat{t}) - \theta. \tag{11}$$

Note that the framework in the previous studies [14,15] corresponds to the case that $H(t)$ is constant.

By using Fourier transform representation of the delta function and the Heaviside step function and by Taylor expansion with respect to $v(t_s)$ and $v'(t_s)$, we obtain the following equation:

$$\begin{aligned} s(\tau) = {} & \frac{1}{4\pi}\int_0^\infty dt_s \int_{-\infty}^{\infty} d\omega \exp[i\omega H(t_s)] \sum_{m=0}^{\infty} \frac{(i\omega)^m}{m!} \\ & \times [a_{m,1}(t_s,\tau) + a_{m,0}(t_s,\tau)H'(t_s)] \\ & + \frac{1}{4\pi^2}\int_0^\infty dt_s \int_{-\infty}^{\infty} d\omega \int_{-\infty}^{\infty} d\nu \frac{\exp[i\omega H(t_s) + i\nu H'(t_s)]}{i\nu} \\ & \times \sum_{m=0}^{\infty}\sum_{n=0}^{\infty} \frac{(i\omega)^m (i\nu)^n}{m!n!}[a_{m,n+1}(t_s,\tau) + a_{m,n}(t_s,\tau)H'(t_s)], \end{aligned} \tag{12}$$

where the correlation $a_{m,n}(t_s,\tau)$ is expressed as follows:

$$a_{m,n}(t_s,\tau) = \langle v^m(t_s)[v'(t_s)]^n \xi(t_s-\tau)\rangle_\xi. \tag{13}$$

To evaluate the STA, we need to calculate the correlations $\{a_{m,n}(t_s,\tau)\}$. It is in principle possible to derive the STA rigorously by evaluating the inverse Fourier transforms of the correlations $\{a_{m,n}(t_s,\tau)\}$ for all possible combinations of m and n. Due to the properties of the white Gaussian noise, the correlation $a_{m,n}(t_s,\tau)$ can be decomposed to

$$a_{m,n}(t_s,\tau) = \kappa(\tau) f_{m,n}(t_s) + \kappa'(\tau) g_{m,n}(t_s), \tag{14}$$

where $f_{m,n}(t_s)$ and $g_{m,n}(t_s)$ are functions of t_s. Thus, the general form of the STA is found to be expressed by a linear combination of the response kernel and its first-order derivative with respect to time:

$$s(\tau) = c_1\kappa(\tau) + c_2\kappa'(\tau), \tag{15}$$

where c_1 and c_2 are constants.

We have shown by moment expansion that the STA of the SRM is a linear combination of the response kernel and its derivative. This result is consistent with that of the previous study using the threshold crossing model [15] (note that the correlation between $\Theta[v'(t_s)]$ and $\delta[v(t_s)]$ is neglected in the approximation in the previous study). As shown in Fig. 1, the SRM has a resetting mechanisms and can treat both sub and suprathreshold regimes, while the membrane potential in the threshold crossing model just fluctuates without any resetting mechanism. Thus, the derived STA of SRM corresponds to the STA of a neuron model that is more biologically plausible.

B. Suprathreshold STA

When the mean of external input current is suprathreshold, we can evaluate the suprathreshold STA by considering the case of a noise of infinitesimal amplitude, since the neuron can fire with only the constant current. Thus the suprathreshold STA can be obtained by finite-order expansions. By expanding the STA up to the first-order terms, we can express $s(\tau)$ as follows:

$$\begin{aligned} s(\tau) = {} & \frac{1}{4\pi}\int_0^\infty dt_s \int_{-\infty}^{\infty} d\omega \exp[i\omega H(t_s)]\{a_{0,1}(t_s,\tau) \\ & + [a_{0,0}(t_s,\tau) + i\omega a_{1,0}(t_s,\tau)]H'(t_s)\} \\ & + \frac{1}{4\pi^2}\int_0^\infty dt_s \int_{-\infty}^{\infty} d\omega \int_{-\infty}^{\infty} d\nu \frac{\exp[i\omega H(t_s) + i\nu H'(t_s)]}{i\nu} \\ & \times \{a_{0,1}(t_s,\tau) + [a_{0,0}(t_s,\tau) + i\omega a_{1,0}(t_s,\tau) \\ & + i\nu a_{0,1}(t_s,\tau)]H'(t_s)\}. \end{aligned} \tag{16}$$

Using the properties of white Gaussian noise, we calculate the correlations $a_{0,0}(t_s,\tau), a_{1,0}(t_s,\tau), a_{0,1}(t_s,\tau)$ in Eq. (16) as follows:

$$a_{0,0}(t_s,\tau) = \langle \xi(t_s-\tau)\rangle_\xi = 0, \tag{17}$$

$$a_{1,0}(t_s,\tau) = \langle v(t_s)\xi(t_s-\tau)\rangle_\xi = \sigma^2\kappa(\tau), \tag{18}$$

$$a_{0,1}(t_s,\tau) = \langle v'(t_s)\xi(t_s-\tau)\rangle_\xi = \sigma^2\kappa'(\tau), \tag{19}$$

where we put $\kappa(0)=0$. By performing further calculations given in Appendix, we express $s(\tau)$ as follows:

$$s(\tau) = \sigma^2\kappa'(\tau)\int_0^\infty dt_s\Theta[H'(t_s)]\delta[H(t_s)] - \sigma^2\kappa(\tau)\int_0^\infty dt_s\delta[H(t_s)]\delta[H'(t_s)]H''(t_s) + \sigma^2\kappa'(\tau)\int_0^\infty dt_s\delta[H(t_s)]\delta[H'(t_s)]H'(t_s). \quad (20)$$

When the constant current is suprathreshold, the neuron fires in a finite time. Thus, the terms in Eq. (20) that include $\delta[H(t_s)]\delta[H'(t_s)]$ become zero and only the first term remains. When we denote the firing time due to the constant input by T, we have $H(T)=0$. Thus, the main term of the suprathreshold STA is derived as the following expression:

$$s(\tau) = \sigma^2\kappa'(\tau)\int_0^\infty dt_s\Theta[H'(t_s)]\delta[H(t_s)] = \sigma^2\kappa'(\tau)\int_0^\infty dt_s\frac{\Theta[H'(t_s)]\delta(t_s-T)}{H'(t_s)} = \sigma^2\frac{\kappa'(\tau)}{H'(T)}. \quad (21)$$

Thus, our analysis reveals that the suprathreshold STA is proportional to the first derivative of the response kernel.

C. Subthreshold STA

When the mean of external input current is subthreshold, the neuron does not fire with only a constant current. We therefore consider the case of a finite-amplitude noise. Since $v(t_s)$ and $v'(t_s)$ take finite values in this case, we need to evaluate $\delta(x)$ and $\Theta(x)$ at $x\neq 0$ in the moment expansion. We need the infinite-order expansion to evaluate the generalized functions $\delta(x)$ and $\Theta(x)$ for $x\neq 0$. Therefore, the subthreshold STA can be evaluated by the infinite-order expansions. Hence, the subthreshold STA is found to be expressed by the linear combination of the response kernel and its first derivative (note that the values of coefficients c_1 and c_2 are undetermined).

$$s(\tau) = c_1\kappa(\tau) + c_2\kappa'(\tau), \quad (22)$$

In general, c_1 and c_2 may have nonzero values.

From the analysis described above, the suprathreshold STA is found to be expressed by the first derivative of the response kernel by means of the lower-order (finite-order) expansion. On the other hand, the subthreshold STA is shown to be expressed by the linear combination of the response kernel and its derivative by means of the infinite-order expansion. This analytical result shows that the shape of STA changes drastically between the sub and suprathreshold regimes; the STA expressed by the linear combination of the response kernel and its derivative changes into the one expressed by only the derivative of the response kernel, as the system approaches to the suprathreshold regime. This suggests that the mathematical structure changes between the sub and suprathreshold regimes.

IV. NUMERICAL SIMULATIONS

In this section, we verify the analytically derived sub and suprathreshold STAs of the SRM by numerical simulations using two kinds of neuron models: the SRM and a multicompartment model with Hodgkin-Huxley type dynamics. In both simulations, the input current is assumed to consist of a constant current and a stochastic current governed by a white Gaussian noise: as in the previous section, $I(t)=I_0+\xi(t)$ for $t\geq 0$. For simplicity, we assume that at $t=0$ the neuron is in a resting state and that the previous firing occurred at $\hat{t}=0$. The STA is calculated numerically by averaging the time series of the stochastic current inducing a spike over multiple trials.

A. Numerical simulations using SRM

In numerical simulations of the SRM, we use two typical examples of the response kernels: the type I and type II response kernels that are shown in Figs. 2(A) and 3(A), respectively. The type I and II response kernels can mimic the subthreshold dynamics of type I and II biologically plausible neuron models [25]. For simplicity, the suprathreshold response kernel $\eta(t)$ is set to be zero. We obtain the STA numerically by calculating the average over 5×10^6 trials.

Figure 2 shows the results for the type I kernel. The type I kernel used here [Fig. 2(A)] is expressed by the following equation:

$$\kappa(t) = \frac{t}{\tau_0}\exp\left(-\frac{t}{\tau_0}\right), \quad (23)$$

where τ_0 is a time constant. We set $I_0=1$ and $\tau_0=1$. In this parameter setting, $H(\infty)$ defined by Eq. (11) becomes $H(\infty)=I_0\int_0^\infty\kappa(s)ds-\theta=1-\theta$. Thus, the condition $H(\infty)>0$ (namely, $\theta<1$) corresponds to the suprathreshold mean stimuli, whereas the condition $H(\infty)<0(\theta>1)$ corresponds to the subthreshold mean stimuli.

We first consider the situation that the mean stimuli are suprathreshold in order to obtain the suprathreshold STA; the firing threshold is set to satisfy $H(\infty)>0$. The STA of the SRM obtained from simulations is shown by cross symbols in Fig. 2(B). As shown in the previous section, we can derive the suprathreshold STA from the response kernel, $\kappa(t)$. The solid line in Fig. 2(B) indicates the STA derived from the type I kernel [Eq. (23)]. We find that the numerically obtained suprathreshold STA is likely to be similar to the first derivative of the type I kernel with respect to time t.

The subthreshold STA, in contrast, has the different profile as shown by crosses in Fig. 2(C). Here we set the firing threshold high enough to satisfy $H(\infty)<0$. The subthreshold STA [Fig. 2(C)] takes positive values over a wider range than does the suprathreshold STA [Fig. 2(B)]. This suggests that the subthreshold STA cannot be expressed by only the first derivative of response kernel. The solid line in Fig. 2(C) is the one fitted by using a linear combination of the kernel itself and its first derivative. We see that the subthreshold STA obtained numerically is fitted well by a linear combination of the kernel and its first derivative, as indicated by Eq. (15). These numerical results obtained by using the SRM

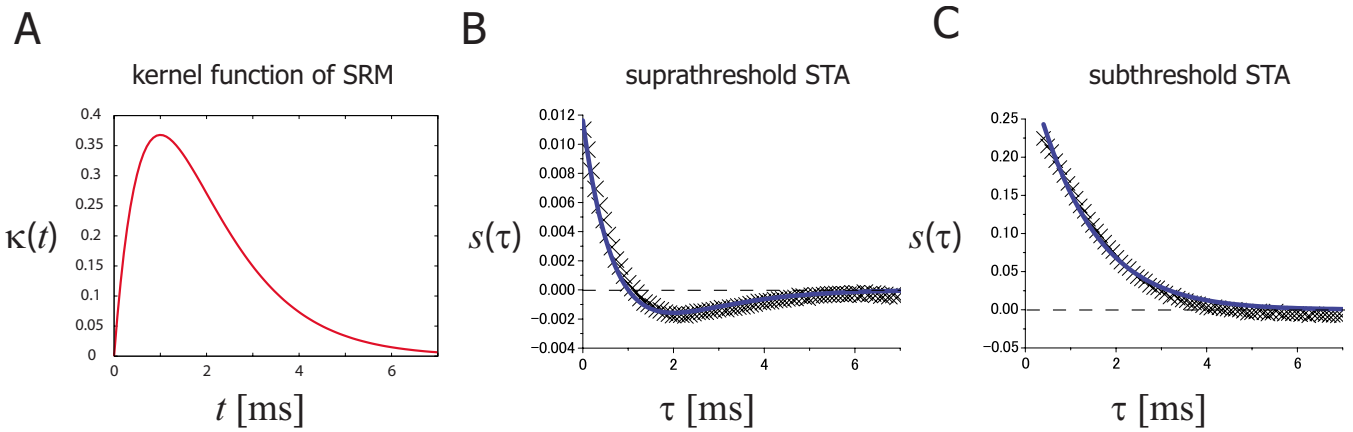

FIG. 2. (Color online) (A) Type I response kernel $\kappa(t)$ of SRM ($\tau_0=1$). (B) Suprathreshold STA obtained in numerical simulation (crosses) and the suprathreshold STA derived from the response kernel of the SRM as the derivative of the kernel $\kappa'(t)$ (solid line). Parameters are set as $\sigma=0.01$, $\theta=0.99$. (C) Subthreshold STA obtained in numerical simulation (crosses). The solid line in C is a line fitted to the numerically obtained subthreshold STA by a linear combination of the response kernel and its first derivative $c_1\kappa(\tau)+c_2\kappa'(\tau)$. Coefficients of the linear combination are determined by the least-squares method ($c_1=0.4156$ and $c_2=0.3274$). Parameters are set as $\sigma=0.1$, $\theta=1.1$.

with the type I kernel show that the shape of STA changes between sub and suprathreshold regimes, as indicated by the analyses in the previous section.

We next show the results for the type II kernel (Fig. 3). The type II kernel is expressed by the following equation [Fig. 3(A)]:

$$\kappa(t)=\frac{t}{\tau_0}\exp\left(-\frac{t}{\tau_0}\right)\cos\left(\frac{t}{\tau_1}\right), \tag{24}$$

where τ_1 is a time constant. The parameters of the response kernel are set as follows: $\tau_0=1$ and $\tau_1=2$.

In order to obtain the suprathreshold STA of the SRM with type II kernel numerically, we first set the firing threshold at a value lower than the maximal membrane potential due to the constant current, which satisfies the condition $\max_t H(t)>0$. We set the parameters of the external input as follows: $I_0=1$ and $\sigma=0.01$. As shown in Fig. 3(B), the STA theoretically derived from the type II kernel is in good agreement with the numerically obtained suprathreshold STA. Thus the suprathreshold STA for the SRM with a type II kernel such as that for the SRM with a type I kernel, can be expressed by the first derivative of the response kernel.

Furthermore, we obtained the subthreshold STA for the SRM with type II kernel numerically by setting the firing threshold to satisfy the condition $\max_t H(t)<0$. The obtained STA is shown by crosses in Fig. 3(C). We see that this numerically obtained STA for the type II response kernel can be fitted by the linear combination of the response kernel $\kappa(\tau)$ and its first-order derivative $\kappa'(\tau)$ [the solid line in Fig. 3(C)].

These numerical results show that, for both the type I and II response kernels, the shape of the STA changes between the sub and suprathreshold regimes as derived in the analysis in the previous section. These results suggest that the ratio between c_1 and c_2 in the expression of STA [$s(\tau)=c_1\kappa(\tau)$

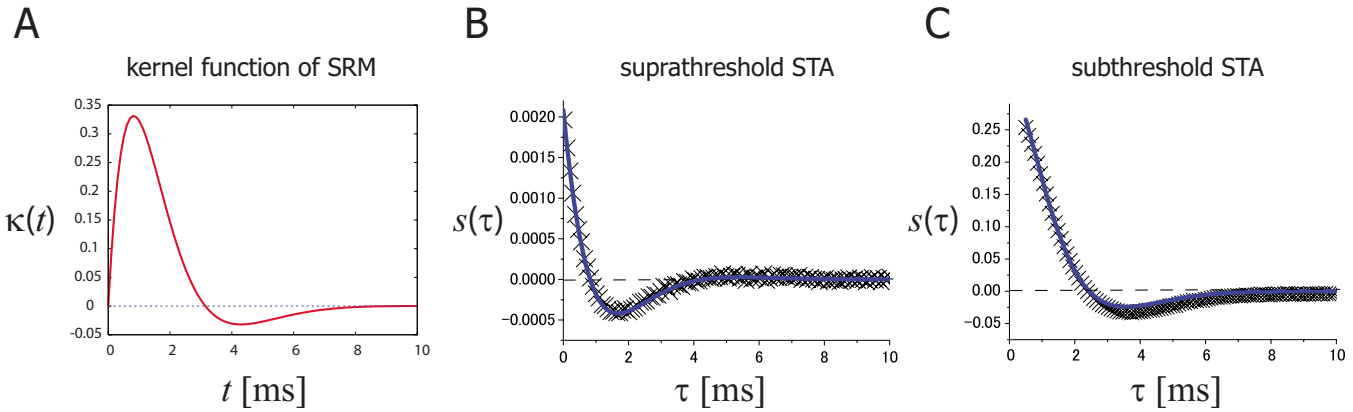

FIG. 3. (Color online) (A) Type II response kernel $\kappa(t)$ of the SRM ($\tau_0=1$, $\tau_1=2$). (B) Suprathreshold STA obtained in numerical simulation (crosses) and the suprathreshold STA derived from the kernel of the SRM as the derivative of the kernel $\kappa'(t)$ (solid line). Parameters are set as $\sigma=0.01$, $\theta=0.55$. (C) Subthreshold STA obtained in numerical simulation (crosses) and a curve fitted to the numerically obtained subthreshold STA by the linear combination of the response kernel and its first derivative (solid line). Coefficients are determined by the least square method ($c_1=0.6456$ and $c_2=0.32$). Parameters are set as $\sigma=0.12$, $\theta=0.6$.

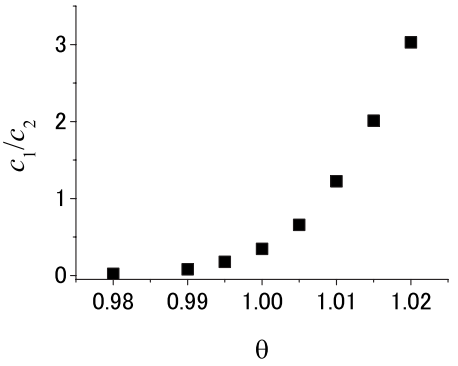

FIG. 4. Dependence of the STA on the firing threshold θ in numerical simulations using the SRM. The numerically obtained STAs for different firing thresholds are fitted by a linear combination of the response kernel and its derivative and the dependence of the ratio between the coefficients c_1/c_2 on the threshold θ is shown. The fitting curve is calculated using the least-squares method. The type I kernel is used, and the noise amplitude is set at σ=0.01. The suprathreshold (subthreshold) regime corresponds to $\theta<1(\theta>1)$.

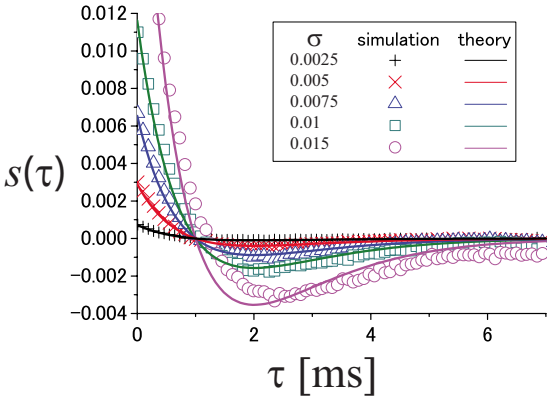

FIG. 5. (Color online) Dependence of the suprathreshold STA of the SRM on noise amplitude (σ). The numerically obtained suprathreshold STA (symbols) is fitted well by the theoretically derived curve for the small amplitudes of noise. This shows that the dependence of STA on noise amplitude derived in our analysis is valid for weak noise. The STA for each noise level is indicated by the following symbols: σ=0.0025 (plus, +), 0.005 (cross, ×), 0.0075 (triangle, △), 0.01 (square, □), 0.015 (circle, ○). The type I kernel is used, and the firing threshold is set at θ=0.99.

$+c_2\kappa'(\tau)]$ changes between the sub and suprathreshold regimes. To verify this, we perform numerical simulations for different firing thresholds by using the SRM with type I response kernel. The dependence of the STA on the firing threshold is shown in Fig. 4. As shown in Fig. 4, the ratio c_1/c_2 takes nearly zero values when $\theta<1$ (i.e., in the suprathreshold regime), whereas c_1/c_2 takes positive values and increases as θ increases when $\theta>1$ (in the subthreshold regime). Note in Fig. 4 that $c_1\neq 0$ for $\theta<1$ because we used noise with a finite amplitude. Our numerical simulations show that, as the mean stimuli increase beyond the suprathreshold regime, the STA expressed by the linear combination of the response kernel and its derivative in the subthreshold regime changed into the STA expressed by only the derivative of the response kernel.

B. Validation of analytical form of suprathreshold STA

Our analysis showed that the main term of the suprathreshold STA of the SRM is proportional to $\sigma^2\kappa'(\tau)$. To validate this analytical form of the suprathreshold STA, we perform numerical simulations to evaluate the dependence of the suprathreshold STA on noise amplitude. Figure 5 shows the numerical results of the STAs for the following five values of noise amplitudes: σ=0.0025, 0.005, 0.0075, 0.01, and 0.015. We also show the suprathreshold STAs derived theoretically from the response kernel for the corresponding five noise levels (solid lines in Fig. 5). One sees that the numerically obtained STAs for different noise levels are fitted well by the theoretically derived STAs for the corresponding noise levels. These results show that the analytical form of the suprathreshold STA is valid and that the dominant term of the suprathreshold STA is proportional to σ^2.

C. Simulations using a compartment model with Hodgkin-Huxley type dynamics

To verify the analytical results for the sub and suprathreshold STAs of the SRM in a more biologically plausible neuron model, we perform numerical simulations using a two-compartment model with somatic and dendritic compartments [Fig. 6(A)]. The external input $I(t)=I_0+\xi(t)$ is assumed to be given to the dendritic compartment, and the STA is calculated as the trial average (over 10^7 trials) of the stochastic current inducing somatic spikes.

The somatic compartment is assumed to have the Hodgkin-Huxley type dynamics with type I excitability proposed by Wang and Buzsáki, as follows [26,28]:

$$C\frac{dV_s}{dt} = -g_{Na}m^3h(V_s-E_{Na}) - g_K n^4(V_s-E_K) - g_L(V_s-E_L) - g_{axial}(V_s-V_d), \quad (25)$$

where V_s and V_d are membrane potentials at the somatic and dendritic compartments, respectively. m and h are activation and inactivation variables of the sodium channel and n is an activation variable of the potassium channel. C is the membrane capacitance, g_{axial} is the axial conductance, and g_x and E_x ($x\in\{Na,K,L\}$) are the maximal conductances and the reversal potentials, respectively. We set g_{axial}=0.1 mS/cm^2 and assume that other parameters and the dynamics for m, h, and n to be the same as in [28]. The dendritic compartment is assumed to have leak and axial currents as well as an external input current $I(t)$ as follows:

$$C\frac{dV_d}{dt} = -g_L(V_d-E_L) - g_{axial}(V_d-V_s) + I(t). \quad (26)$$

To obtain a subthreshold kernel of the multicompartment model, we give an impulse stimulation to the dendritic compartment. The impulse stimulation is set to be sufficiently weak not to induce an action potential. The response kernel obtained as the impulse response at the somatic compartment is shown in Fig. 6(B) and the suprathreshold STA derived from the response kernel is shown in Fig. 6(C). We also

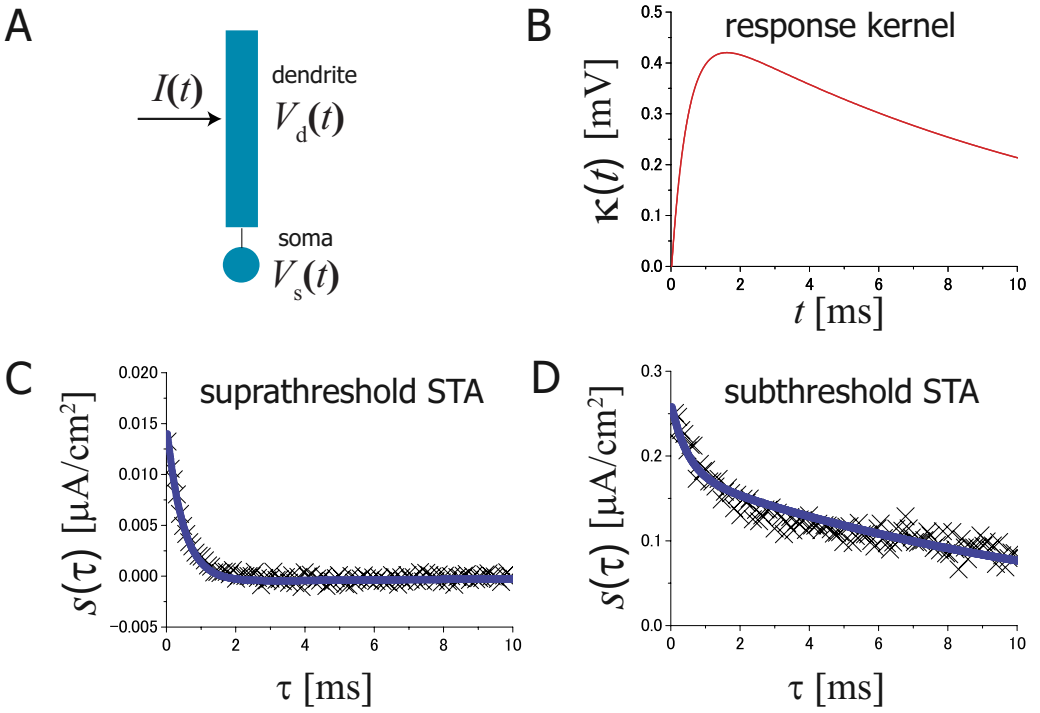

FIG. 6. (Color online) (A) Schematic diagram of a multicompartment model with Hodgkin-Huxley type dynamics. The external inputs are given to a dendritic compartment. (B) Impulse response (corresponding to response kernel) obtained from numerical simulation. (C) Suprathreshold STA derived analytically as a first-order derivative of the response kernel shown in B (solid line) and the suprathreshold STA obtained directly by numerical simulations using the multicompartment model (crosses). (D) Subthreshold STA fitted using a linear combination of the response kernel shown in B and its derivative (solid line) to the numerically obtained subthreshold STA (crosses).

obtain the suprathreshold STA directly by numerical simulation. The constant current is set at a suprathreshold level (I_0=1 μA/cm^2 and σ=0.05 μA/cm^2). The crosses in Fig. 6(C) show the suprathreshold STA obtained numerically. We find that the STA obtained numerically has a profile similar to that of the STA obtained analytically. Thus, we see that the analytically derived relationship between the suprathreshold STA and SRM holds even in multicompartment model with Hodgkin-Huxley type dynamics. To obtain the subthreshold STA numerically, we perform numerical simulations in which the mean of external input is set to a subthreshold level (I_0=0.6 μA/cm^2, σ=0.1 μA/cm^2). The numerically obtained STA is shown by crosses in Fig. 6(D), where we see that the subthreshold STA is fitted well by the linear combination of the subthreshold response kernel and its derivative [Fig. 6(D), solid line]. These results show that the difference in the time profile between the subthreshold STA and suprathreshold STA, which has been derived in our analysis, occurs even in the multicompartment model with Hodgkin-Huxley type dynamics.

V. CONCLUDING REMARKS

In this study, we have analytically derived the relation between the response kernel of the SRM and the STA by moment expansion. By our analysis, the change in the time profile between the sub and suprathreshold STAs has been verified. We first showed analytically that the general form of the STA can be expressed by a linear combination of the response kernel and its derivative $[s(\tau)=c_1\kappa(\tau)+c_2\kappa'(\tau)]$. We showed by the lower-order moment expansion that the coefficient of the response kernel (c_1) in the linear combination was zero for the suprathreshold mean stimuli, leading to a theoretical finding that the dominant term of the suprathreshold STA can be expressed by only the first derivative of the response kernel. On the other hand, the infinite-order moment expansion implied that c_1 is a nonzero value for the subthreshold mean stimuli, indicating that the subthreshold STA can be expressed as a linear combination of the response kernel and its derivative. To verify the difference between the sub and suprathreshold STAs, we performed numerical simulations using a multicompartment model with Hodgkin-Huxley type dynamics. Numerical results showed that the switch of the STA between the sub and suprathreshold regimes that was derived in our analyses also occurs in a multicompartment model.

Mato and Samengo [20] numerically showed the difference between sub and suprathreshold STAs by relating those STAs to the PRC, which can be defined when the mean stimuli are suprathreshold. From their numerical results, the suprathreshold STA was found to be similar to the first derivative of the PRC, whereas the subthreshold STA was found to be similar to the PRC. In the present study, on the other hand, we have analytically shown the difference between sub and suprathreshold STAs by relating those STAs to the response kernel, which can be defined regardless of whether the mean stimuli are sub or suprathreshold.

Ermentrout *et al.* [13] analytically showed using the phase oscillator model that the suprathreshold STA is proportional

to the first derivative of the PRC. Although the formulation using the SRM in the present study is related to that using the phase oscillator model in the previous study [13], these formulations are different from each other in whether the first passage time problem is treated; the present study explicitly treated the first passage time problem whereas the previous study [13] did not. By taking the first passage time problem into account, we showed that the suprathreshold STA obtained from a neuron model including the nonlinear effect through Eq. (8) is similar to the one obtained from the phase oscillator model.

The PRC can be derived theoretically by means of the adjoint method based on the local linearization of the dynamical equation of a neuron model around its limit-cycle orbit, while the PRC can be obtained heuristically as an impulse response from both model and biological neurons in the periodic firing. On the other hand, the response kernel of the SRM can be derived theoretically by means of the linearization of the dynamical equation of a neuron model around its resting state, while the response kernel can be obtained heuristically as an impulse response from both model and biological neurons in the resting state [25]. Therefore, both the PRC and the response kernel can be derived theoretically from the dynamical equations of a neuron model such as the conductance-based model, whereas both can be obtained experimentally from biological neurons.

In the present study, we assumed that the stochastic current $\xi(t)$ is described by the white Gaussian noise. This assumption may be too strict for some physiological situations. Using the formulation given in the present study, we can investigate the case of the colored noise. We leave this as a future work.

In the previous study by Burak *et al.* [15], the subthreshold STA of the threshold crossing model was analytically shown to be a linear combination of the response kernel and its derivative. In their analysis, $v(t_s)$ and $v'(t_s)$ in the factor $\Theta[v'(t_s)]\delta[v(t_s)]$ given in Eqs. (8) and (10) were assumed to be uncorrelated, approximately. In the present study, we also showed that the subthreshold STA is expressed by a linear combination of the response kernel and its derivative. However, in the present paper, the coefficients in linear combination in the subthreshold STA have not been determined yet, while the suprathreshold STA was successfully derived including the coefficient. Since the coefficients in the STA determine the encoding properties of single neurons, it is important to determine the coefficients of the subthreshold STA rigorously. We leave the evaluation of the coefficients of the subthreshold STA by using the infinite-order expansion as a future work.

ACKNOWLEDGMENTS

This work was partially supported by Grants-in-Aid for Scientific Research (Grants No. 20509001 for T.O., Grant No. 20500201 for T.A., and Grants No. 18079003, No. 20240020, and No. 20650019 for M.O.) from Ministry of Education, Culture, Sports, Science and Technology, Japan.

APPENDIX: DETAILED CALCULATION IN LOWER-ORDER MOMENT EXPANSION

In this Appendix, we describe the derivation of Eq. (20) from Eqs. (16)–(19) by lower-order moment expansions of the STA. That is, we evaluate the following expression:

$$\begin{aligned} s(\tau) = {} & \frac{1}{4\pi}\int_0^\infty dt_s \int_{-\infty}^\infty d\omega \exp[i\omega H(t_s)]\{a_{0,1}(t_s,\tau) \\ & + [a_{0,0}(t_s,\tau) + i\omega a_{1,0}(t_s,\tau)]H'(t_s)\} \\ & + \frac{1}{4\pi^2}\int_0^\infty dt_s \int_{-\infty}^\infty d\omega \int_{-\infty}^\infty d\nu \frac{\exp[i\omega H(t_s) + i\nu H'(t_s)]}{i\nu} \\ & \times \{a_{0,1}(t_s,\tau) + [a_{0,0}(t_s,\tau) + i\omega a_{1,0}(t_s,\tau) \\ & + i\nu a_{0,1}(t_s,\tau)]H'(t_s)\}. \end{aligned} \tag{A1}$$

Using $a_{0,0}(t_s,\tau)=0$, $a_{1,0}(t_s,\tau)=\sigma^2\kappa(\tau)$, and $a_{0,1}(t_s,\tau)=\sigma^2\kappa'(\tau)$ given in Eqs. (17)–(19), we express Eq. (A1) as follows:

$$\begin{aligned} s(\tau) = {} & \frac{\sigma^2}{4\pi}\int_0^\infty dt_s \int_{-\infty}^\infty d\omega \exp[i\omega H(t_s)][\kappa'(\tau) + i\omega\kappa(\tau)H'(t_s)] \\ & + \frac{\sigma^2}{4\pi^2}\int_0^\infty dt_s \int_{-\infty}^\infty d\omega \int_{-\infty}^\infty d\nu \frac{\exp[i\omega H(t_s) + i\nu H'(t_s)]}{i\nu} \\ & \times \{\kappa'(\tau) + [i\omega\kappa(\tau) + i\nu\kappa'(\tau)]H'(t_s)\}. \end{aligned} \tag{A2}$$

By expanding this expression, we obtain

$$\begin{aligned} s(\tau) = {} & \frac{\sigma^2\kappa'(\tau)}{4\pi}\int_0^\infty dt_s \int_{-\infty}^\infty d\omega \exp[i\omega H(t_s)] + \frac{\sigma^2\kappa(\tau)}{4\pi}\int_0^\infty dt_s \int_{-\infty}^\infty d\omega \exp[i\omega H(t_s)]i\omega H'(t_s) + \frac{\sigma^2\kappa'(\tau)}{4\pi^2}\int_0^\infty dt_s \int_{-\infty}^\infty d\omega \int_{-\infty}^\infty d\nu \\ & \times \frac{\exp[i\omega H(t_s) + i\nu H'(t_s)]}{i\nu} + \frac{\sigma^2\kappa(\tau)}{4\pi^2}\int_0^\infty dt_s \int_{-\infty}^\infty d\omega \int_{-\infty}^\infty d\nu \frac{\exp[i\omega H(t_s) + i\nu H'(t_s)]}{i\nu} i\omega H'(t_s) \\ & + \frac{\sigma^2\kappa'(\tau)}{4\pi^2}\int_0^\infty dt_s \int_{-\infty}^\infty d\omega \int_{-\infty}^\infty d\nu \exp[i\omega H(t_s) + i\nu H'(t_s)]H'(t_s) \\ = {} & \sigma^2\kappa'(\tau)\int_0^\infty dt_s \left\{\frac{1}{2} + \frac{1}{2\pi}\int_{-\infty}^\infty d\nu \frac{\exp[i\nu H'(t_s)]}{i\nu}\right\}\frac{1}{2\pi}\int_{-\infty}^\infty d\omega \exp[i\omega H(t_s)] + \sigma^2\kappa(\tau)\int_0^\infty dt_s \end{aligned}$$

$$\times\left\{\frac{1}{2}+\frac{1}{2\pi}\int_{-\infty}^{\infty}d\nu\frac{\exp[i\nu H'(t_s)]}{i\nu}\right\}\frac{1}{2\pi}\int_{-\infty}^{\infty}d\omega\exp[i\omega H(t_s)]i\omega H'(t_s)+\sigma^2\kappa'(\tau)\int_0^{\infty}dt_s\frac{1}{2\pi}\int_{-\infty}^{\infty}d\omega$$

$$\times\exp[i\omega H(t_s)]\frac{1}{2\pi}\int_{-\infty}^{\infty}d\nu\exp[i\nu H'(t_s)]H'(t_s). \tag{A3}$$

Since Eq. (A3) includes the Fourier transform representations of the delta function and the Heaviside function, we have

$$s(\tau)=\sigma^2\kappa'(\tau)\int_0^{\infty}dt_s\Theta[H'(t_s)]\delta[H(t_s)]+\sigma^2\kappa(\tau)\int_0^{\infty}dt_s\Theta[H'(t_s)]\frac{d}{dt_s}\delta[H(t_s)]+\sigma^2\kappa'(\tau)\int_0^{\infty}dt_s\delta[H(t_s)]\delta[H'(t_s)]H'(t_s). \tag{A4}$$

By partial integration of the second term in Eq. (A4), we get

$$\sigma^2\kappa(\tau)\int_0^{\infty}dt_s\Theta[H'(t_s)]\frac{d}{dt_s}\delta[H(t_s)]=-\sigma^2\kappa(\tau)\int_0^{\infty}dt_s\delta[H'(t_s)]H''(t_s)\delta[H(t_s)]. \tag{A5}$$

From Eqs. (A4) and (A5), we derive Eq. (20) as follows:

$$s(\tau)=\sigma^2\kappa'(\tau)\int_0^{\infty}dt_s\Theta[H'(t_s)]\delta[H(t_s)]-\sigma^2\kappa(\tau)\int_0^{\infty}dt_s\delta[H(t_s)]\delta[H'(t_s)]H''(t_s)+\sigma^2\kappa'(\tau)\int_0^{\infty}dt_s\delta[H(t_s)]\delta[H'(t_s)]H'(t_s). \tag{A6}$$

[1] E. De Boer and P. Kuyper, IEEE Trans. Biomed. Eng. **BME–15**, 169 (1968).
[2] H. L. Bryant and J. P. Segundo, J. Physiol. **260**, 279 (1976).
[3] F. Rieke, D. Warland, R. de Reyter van Steveninck, and W. Bialek, *Spikes: Exploring the Neural Code* (MIT University Press, Cambridge, MA, 1997).
[4] E. J. Chichilnisky, Network: Comput. Neural Syst. **12**, 199 (2001).
[5] P. Dayan and L. F. Abbott, *Theoretical Neuroscience: Computational and Mathematical Modeling of Neural Systems* (MIT University Press, Cambridge, MA, 2001).
[6] B. Agüera y Arcas and A. L. Fairhall, Neural Comput. **15**, 1789 (2003).
[7] E. P. Simoncelli, L. Paninski, J. Pillow, and O. Schwartz, in *The New Cognitive Neurosciences*, 3rd ed., edited by M. Gazaniga (MIT University Press, Cambridge, MA, 2004).
[8] F. Grenier, I. Timofeev, and M. Steriade, Proc. Natl. Acad. Sci. U.S.A. **95**, 13929 (1998).
[9] P. Fries, J. H. Reynolds, A. E. Rorie, and R. Desimone, Science **291**, 1560 (2001).
[10] R. Segev, J. Goodhouse, J. Puchalla, and M. J. Berry II, Nat. Neurosci. **7**, 1155 (2004).
[11] K. Farrow, J. Haag, and A. Borst, Nat. Neurosci. **9**, 1312 (2006).
[12] L. Paninski, Network Comput. Neural Syst. **14**, 437 (2003).
[13] G. B. Ermentrout, R. F. Galán, and N. N. Urban, Phys. Rev. Lett. **99**, 248103 (2007).
[14] S. Hong, B. Aguera y Arcas, and A. Fairhall, Neural Comput. **19**, 3133 (2007).
[15] Y. Burak, S. Lewallen, and H. Sompolinsky, Neural Comput. (to be published).
[16] L. Paninski, Neural Comput. **18**, 2592 (2006).
[17] W. Gerstner, Neural Netw. **14**, 599 (2001).
[18] L. Badel, W. Gerstner, and M. J. E. Richardson, Neurocomputing **69**, 1062 (2006).
[19] L. Badel, W. Gerstner, and M. J. E. Richardson, Phys. Rev. E **78**, 011914 (2008).
[20] G. Mato and I. Samengo, Neural Comput. **20**, 2418 (2008).
[21] G. B. Ermentrout and N. Kopell, SIAM J. Appl. Math. **46**, 233 (1986).
[22] F. C. Hoppendsteadt and E. M. Izhikevich, *Weakly Connected Neural Networks* (Springer-Verlag, New York, 1997).
[23] W. Gerstner and J. L. van Hemmen, Network **3**, 139 (1992).
[24] W. Gerstner and W. M. Kistler, *Spiking Neuron Models: Single Neurons, Population, Plasticity* (MIT University Press, Cambridge, MA, 2002).
[25] W. Kistler, W. Gerstner, and J. L. H. Hemmen, Neural Comput. **9**, 1015 (1997).
[26] A. L. Hodgkin and A. F. Huxley, J. Physiol. **117**, 500 (1952).
[27] H. C. Tuckwell, *Nonlinear and Stochastic Theories*, Introduction to Theoretical Neurobiology(Cambridge University Press, New York, NY, 1988), Vol. 2.
[28] X.-J. Wang and G. Buzsáki, J. Neurosci. **16**, 6402 (1996).